MEDICAL SCIENCE MONITOR

ANIMAL STUDY

e-ISSN 1643-3750
© Med Sci Monit, 2016; 22: 3062-3072
DOI: 10.12659/MSM.897270

Received: 2015.12.25
Accepted: 2016.02.01
Published: 2016.08.30

Association of Bactericidal Dysfunction of Paneth Cells in Streptozocin-Induced Diabetic Mice with Insulin Deficiency

Authors' Contribution:
Study Design A
Data Collection B
Statistical Analysis C
Data Interpretation D
Manuscript Preparation E
Literature Search F
Funds Collection G

BCE Tao Yu
ABCE Hong-Sheng Yang
C Xi-Ji Lu
F Zhong-Sheng Xia
B Hui Ouyang
B Ti-Dong Shan
C Can-Ze Huang
AG Qi-Kui Chen

Department of Gastroenterology, Sun Yat-Sen Memorial Hospital, Sun Yat-Sen University, Guangzhou, Guangdong, P.R. China

Corresponding Authors: Qi-Kui Chen, e-mail: qikuichen@yahoo.com; Hong-Sheng Yang, e-mail: hensonyang@foxmail.com
Source of support: This study was supported by National Natural Science Foundation of China (No.81270442 and No. 81370475)

Background: Type 1 diabetes mellitus (T1DM) is associated with increased risks of enteric infection. Paneth cells constitute the first line of the gut defense. Little is known about the impact of T1DM on the bactericidal function of intestinal Paneth cells.

Material/Methods: A T1DM mouse model was induced by intraperitoneal injection of streptozocin. The analysis of intestinal microbiota and the mucosal bactericidal assay were conducted to evaluate intestinal innate defense. Numbers of Paneth cells and their expression of related antimicrobial peptides were analyzed. Expression of total insulin receptor (IR) mRNA and relative levels of IR-A/IR-B were analyzed. The primary mouse small intestinal crypt culture was used to analyze the effect of insulin and glucose on the expression of related antimicrobial peptides of Paneth cells.

Results: In T1DM mice, bacterial loads were increased and there was an alteration in the composition of the intestinal microflora. Exogenous bacteria had better survival in the small bowel of the T1DM mice. The expression of Paneth cell-derived antimicrobial peptides was significantly decreased in the T1DM mice, although the number of Paneth cells was increased. Relative levels of IR-A/IR-B in Paneth cells of diabetic mice were elevated, but the total IR mRNA did not change. Insulin treatment restored the expression of antimicrobial peptides and normalized the microbiota in the gut of T1DM mice. Subsequently, *in vitro* culture assay demonstrated that insulin rather than glucose was essential for the optimal expression of Paneth cell-derived antimicrobial peptides.

Conclusions: The bactericidal function of intestinal Paneth cells was impaired in STZ-induced diabetic mice, resulting in the altered intestinal flora, and insulin was essential for the optimal expression of Paneth cell-derived antimicrobial peptides.

MeSH Keywords: **Diabetes Mellitus, Type 1 • Insulin, Isophane • Microbiota • Paneth Cells**

Abbreviations: **T1DM** – type 1 diabetes mellitus; **Lyz** – lysozyme; **Crp** – cryptdin; **TCF4** – transcription factor 4; **STZ** – streptozotocin; **NPH insulin** – Neutral Protamine Hagedorn insulin; **ELISA** – enzyme-linked immunosorbent assay; **PBS** – phosphate-buffered saline; **FACS** – fluorescence-activated cell sorting; **LPS** – lipopolysaccharide; **IR** – insulin receptor; **Mmp7** – matrix metallopeptidase 7

Full-text PDF: http://www.medscimonit.com/abstract/index/idArt/897270

4047 1 7 43

Indexed in: [Current Contents/Clinical Medicine] [SCI Expanded] [ISI Alerting System] [ISI Journals Master List] [Index Medicus/MEDLINE] [EMBASE/Excerpta Medica] [Chemical Abstracts/CAS] [Index Copernicus]

Background

Type 1 diabetes mellitus (T1DM) is a clinical syndrome associated with deficiency of insulin secretion. A mounting body of epidemiological and clinical evidence has shown that patients with T1DM are more susceptible to enteric pathogens, such as enteric bacteria, enterovirus, and fungi, which may cause asymptomatic or symptomatic enteric infections [1–3]. Intestinal innate immune mechanisms play an important role in protection of the host mucosa [4]. The gut innate immune response in T1DM has not been explored mechanistically, although the intestinal epithelium is directly and continually exposed to a diverse array of luminal microbes.

Paneth cells produce and secret antimicrobial peptides, including lysozyme (Lyz) and cryptdins (Crps). They help to shape the composition of the endogenous flora in the gut, limit the numbers of microbes colonizing the crypts and lumen, and protect stem cells in the niche against pathogens [5,6]. Researches indicated that impaired Paneth cell function might be responsible for the increased susceptibility to enteric infection [7–9]. On the other hand, increased expression of Crps, a potent antimicrobial peptide, in Paneth cells protected mice from orally administered challenges with an enteric pathogen [10]. Paneth cells clearly play a crucial role in the gut defense.

Insulin plays an important role in intestinal epithelial self-renewal and differentiation by coordination of Wnt signaling activities [11–14]. Wnt signaling, which can be transduced through β-catenin/transcription factor 4 (TCF4), helps maintain a stem cell/progenitor phenotype, and also induces positioning, differentiation, and maturation of Paneth cells in intestinal crypts [15–18]. Insulin signaling is capable of stimulating the expression of Wnt pathway component TCF4 in intestinal epithelial cells [13]. Thus, insulin may participate in the differentiation and maturation of Paneth cells. However, it has been unclear whether insulin deficiency can lead to alteration of Paneth cells in people with T1DM.

We hypothesized that decreased level of insulin downregulate production of antimicrobial peptides of Paneth cells, leading to susceptibility to enteric infection in people with T1DM. To examine this possibility, we investigated the bactericidal function of Paneth cells in control mice and in insulin-treated and untreated streptozotocin (STZ)-induced diabetic mice. Primary small intestinal crypt culture was used to analyze the effect of insulin and glucose on the expression of related antimicrobial peptides of Paneth cells.

Material and Methods

Animals and STZ-induced diabetic mouse model

C57BL/6J mice (8 weeks old) from the Laboratory Animal Center of Sun Yat-Sen University (Guangzhou, China) were used. All animal experiments were approved by the Animal Care Committee of Sun Yat-Sen University (permit number: 201412000091). A diabetic mouse model was induced by daily intraperitoneal injection of STZ (Sigma, USA; 70 mg/kg) for 5 days [19,20]. The control mice were injected intraperitoneally with vehicle. Mice with random blood glucose levels in excess of 16.7 mM were considered to be diabetic mice. Diabetic mice were divided randomly into 2 groups: the UDM group (untreated diabetic mice) served as the diabetic control and only received vehicle, whereas the IDM group (insulin-treated diabetic mice) was treated with 0.08 IU neutral protamine Hagedorn insulin (NPH insulin, Novo Nordisk A/S, Denmark) subcutaneously twice daily for 12 weeks [21,22]. The mice were sacrificed under ether anesthesia at the end of the experiment.

Enzyme-link immunosorbent assays (ELISAs)

At week 14, blood was collected by cardiac puncture and was centrifuged at 2000× gravity at 4°C for 15 min. Plasma insulin levels were determined by ELISA kit (Merk Millipore, USA) per manufacturer instructions.

Isolation of microbial genomic DNA and real-time PCR for microbiota analysis

Intraluminal contents in the distal intestine were collected. Microbial genomic DNA was isolated using the QIAamp DNA Stool Mini Kit (Qiagen, Germany). The relative abundance of total bacteria and specific intestinal microbiota was measured by real-time PCR using taxon-specific 16s rDNA primers on a CFX Connect™ real-time PCR detection system (Bio-Rad, USA) as previously described [23,24]. Real-time PCR was conducted in a volume of 25 µl containing 10 ng of luminal DNA and 300 nmol/l of each 16S rRNA gene-targeted primer. The primers are shown in Table 1. Results of total bacterial quantity were corrected for weight of intraluminal contents. The abundance of *Firmicute* and *Bacteroidetes* in the luminal contents is presented relative to the total bacterial abundance.

Intestinal bactericidal activity *in vivo*

The protocol was previously described by Wilson et al. [7]. Mice were orally infected at week 14. *Escherichia coli* K12 ER2738 (*E. coli* K12, New England Biolabs, USA), a tetracycline-resistant bacterial strain, was incubated in 150 ml of LB broth containing tetracycline (20 mg/l; Sigma-Aldrich, USA) for 48 h at 37°C. Bacteria were pelleted and suspended in 1.5 ml of

Indexed in: [Current Contents/Clinical Medicine] [SCI Expanded] [ISI Alerting System] [ISI Journals Master List] [Index Medicus/MEDLINE] [EMBASE/Excerpta Medica] [Chemical Abstracts/CAS] [Index Copernicus]

Table 1. The primer sequences for PCR.

Gene	Forward or reverse	Primer sequence
Crps	Forward	5'-GGT GAT CAT CAG ACC CCA GCA TCA GT-3'
	Reverse	5'-AAG AGA CTA AAA CTG AGG AGC AGC-3'
Mmp7	Forward	5'-GGT GTG GAG TGC CAG ATG TT-3'
	Reverse	5'-TAT CCG CAG TCC CCC AAC TA-3'
Lyz1	Forward	5'-CAG CTC ACT AGT CGC TCC TG-3'
	Reverse	5'-TAG AGC TGC CCC TTT CAT CT-3'
IR	Forward	5'-CAA TGG GAC CAC TGT ATG CAT CT-3'
	Reverse	5'-GTC CGG CAC GTA CAC AGA AGA-3'
18S rRNA	Forward	5'-GCT AGG AAT AAT GGA ATA GG-3'
	Reverse	5'-ACT TTC GTT CTT GAG GAA TG-3'
Bact	Forward	5'-CRA ACA GGA TTA GAT ACC CT-3'
	Reverse	5'-GGT AAG GTT CCT CGC GTA T-3'
Firm	Forward	5'-TGA AAC TYA AAG GAA TTG ACG-3'
	Reverse	5'-ACC ATG CAC CAC CTG TC-3'
Univ	Forward	5'-AAA CTC AAA KGA ATT GAC GG-3'
	Reverse	5'-CTC ACR RCA CGA GCT GAC-3'

Crps – mouse general cryptdins; Mmp7 – mouse matrix metallopeptidase 7; Lyz1 – mouse lysozyme 1; IR – mouse total insulin receptor; 18S rRNA – mouse 18S ribosomal RNA; Bact – *Bacteroidetes*; Firm – *Firmicutes*; Univ – *Universal*.

phosphate-buffered saline (PBS). Mice were given 0.1 ml of 0.1 M sodium bicarbonate, immediately followed by a 0.1 ml bolus of bacteria (1–2×10^{10} CFUs) in PBS. After 3 h, the intestine was harvested and cut into 2 segments of equal length. Each segment was homogenized in 3 ml of PBS and serially diluted for plating on LB media containing tetracycline (20 mg/l) for determination of CFUs per milliliter.

Immunohistochemical analysis

Epitopes were retrieved using boiled 0.01 M citrate buffer (pH 6.0). All sections were incubated with anti-mouse Lyz antibody (1: 2,500; Abcam, USA) diluted with PBS at 4°C overnight, and then incubated with EnVision+/HRP/Rb (DAKO, Denmark) for 30 min. The sections were incubated in 3, 3'- diaminobenzidine tetrahydrochloride (Maxin, China) for 5 min and then counterstained with hematoxylin for 30 s.

Isolation of primary intestinal epithelial cells

Isolation of small intestinal crypts or villi was performed as previously described [25]. Briefly, the intestinal segment was everted and incubated in the dissociation reagent (30 mM EDTA, 1.5 mM DTT in PBS) at 37°C for 20 min. Crypts or villi were isolated by several rapid bursts of vibration. Crypts were discriminated from villi with specific appearance of Paneth cell granules.

Fluorescence-activated cell sorting (FACS)

Isolated intestinal crypts were re-suspended in Hank's balanced salt solution/0.3 U/ml dispase at 37°C. DNase I (50 μg/ml) was added, and the cells were sequentially passed through 70-μm and 40-μm filters. Cells were incubated with CD24-PE antibody (BD Pharmingen, USA) at 0.25 μg per 1×10^6 cells in 100 μl PBS/1% BSA for 15 min at room temperature, washed with PBS/1% BSA, and analyzed in a FACSJazz machine (BD Bioscience, USA). Doublets were excluded using a bivariate plot of pulse width *vs.* forward scatter. Hematopoietic cells were excluded using side-scatter/forward-scatter gating that had previously been optimized to exclude all $CD45^+$ cells from epithelial preparations [26]. The $CD24^{high}SSC^+$ cell population was sorted using the FACSJazz machine as described in previous studies [27]. All data analysis was performed using FlowJo V10 software (Treestar Inc., USA).

RNA isolation and quantitative real-time RT-PCR

Total RNA from samples was extracted by using TRIzol® Reagent (Life Technologies Corporation, USA). RNA was reverse

Indexed in: [Current Contents/Clinical Medicine] [SCI Expanded] [ISI Alerting System] [ISI Journals Master List] [Index Medicus/MEDLINE] [EMBASE/Excerpta Medica] [Chemical Abstracts/CAS] [Index Copernicus]

transcribed with PrimeScript™ RT Master Mix (TaKaRa Bio, Japan). Real-time PCR was performed using SYBR® Premix Ex Taq™ (TaKaRa Bio, Japan) on a CFX Connect™ real-time PCR detection system (Bio-Rad, USA). The primers (forward and reverse) are shown in Table 1. The primers used to amplify total Crp genes were designed by Gulati et al. [28]. Data were analyzed using the ΔΔCt method with 18S ribosomal RNA as the constitutive marker.

Western blotting analysis

Isolated crypt samples were incubated in RIPA buffer (Thermo Scientific, USA). The protein sample was separated by 12% SDS-PAGE and transferred to PVDF membranes. The membranes were probed with the following primary antibodies overnight at 4°C: rabbit anti-mouse Lyz antibody (1:25,000; Abcam, UK), and rabbit anti-mouse β-actin antibody (1:2000; Cell Signaling Technology, USA). Then, incubation with antibody against rabbit (1:5000; Cell Signaling Technology, USA) was conducted for 1 h at room temperature. The integrated intensity for the protein bands was determined by scanning densitometry and analyzed with Glyko BandScan 5.0. The data were analyzed using relative intensity with β-actin as the constitutive marker.

Stimulation of Paneth cell secretion and bactericidal activity assay

Preparations of 2000 intact individual crypts or 500 sheets of villus enterocytes were incubated at 37°C for 30 min in 2 ml of iPIPES buffer, consisting of 10 mM PIPES (pH 7.4; Sigma-Aldrich, USA) and 137 mM NaCl, with the Toll-like receptor 4 agonist lipopolysaccharide (LPS; purified from *Escherichia coli* 0111: B4, 10 μg/ml; Sigma-Aldrich, USA). After incubation, the supernatant was collected for bactericidal assay. In triplicate, 5×10^6 CFUs *E. coli* K12 were incubated for 1 h at 37°C in 50 μl iPIPES with 10 μl of samples or 60 μl iPIPES alone as a control in individual experiments. Surviving CFUs were quantified by growth on LB media containing tetracycline (20 mg/l; Sigma-Aldrich, USA) at 37°C overnight. CFUs were normalized to control plates and results are expressed as bactericidal activity as measured by the reduction in percent CFUs.

RT-PCR for insulin receptor (IR) isoforms

The experiment was conducted according to the method of Ulanet et al. [29]. RT-PCR was performed using a PrimeScript™ 1st Strand cDNA Synthesis kit (TaKaRa, Japan) and TaKaRa Ex Taq HS (TaKaRa, Japan) in PCR buffer and 0.5 μM dNTPs. The primer sequences of IR isoforms were: upstream: 5'-AAT CAG AGT GAG TAT GAC GAC-3'; downstream: 5'-GAC TTG TGG GCA CAA TGG TA-3'. The integrated intensity for the bands was analyzed with Glyko BandScan 5.0.

Culture of primary small intestinal crypts

Culture experiments were carried out using methods previously described [30]. Isolated crypts from the small intestines of 8-week-old C57BL/6 mice were plated at the density of 300 crypts per 50 μl and cultured in growth factor-reduced Matrigel™ (BD Biosciences, USA) with a standard growth factor cocktail (EGF: 50 ng/ml, R&D Systems, USA; Noggin: 100 ng/ml, PeproTech, USA; R-Spondin 1:1 μg/ml, R&D Systems, USA). On the fifth day of culture, crypt organoids were administrated with glucose, mannitol, and/or insulin at different concentrations for 8 h.

Statistical analysis

Results are expressed as mean ± standard error. Comparisons between different treatment groups were performed by ANOVA followed by the Bonferroni post hoc test. When data were not normally distributed, the Kruskal-Wallis test was utilized to compare means, followed by Dunn's multiple comparison testing. Statistical analyses were carried out using the GraphPad Prism 4 software package (GraphPad Software Inc., USA). Differences were considered significant at $P<0.05$.

Results

Blood glucose and plasma insulin levels of the control, IDM, and UDM group

After 5 days of STZ injection, the blood glucose of diabetic mice was significantly higher than that in the control mice at week 2 (n=20, $P<0.05$; Figure 1A). The blood glucose in the IDM group decreased to the level of the control group at week 4. The blood glucose of the UDM group remained significantly higher than that in the control and IDM group for 12 weeks (n=20, $P<0.05$; Figure 1A). The UDM group showed significantly lower body weight than the control and IDM groups by 6 weeks (n=20, $P<0.05$; Figure 1B). At week 14, the UDM group exhibited decreased plasma insulin compared with the control and IDM groups (n=20, $P<0.05$; Figure 1C).

Intestinal bacterial load and microbial communities in diabetic mice

The total bacterial number per gram of luminal content in the UDM group was significantly higher than that in the control and the IDM group (n=8, $P<0.05$; Figure 2A). Compared to the control group, the abundance of *Bacteroidetes* was significantly higher and *Firmicute* dominance was less in the UDM group (n=8, $P<0.05$; Figure 2B, 2C). The control group and the IDM group had similar proportions of *Bacteroidetes* and *Firmicutes*. These data indicate that there was gut microflora dysbiosis in

Indexed in: [Current Contents/Clinical Medicine] [SCI Expanded] [ISI Alerting System] [ISI Journals Master List] [Index Medicus/MEDLINE] [EMBASE/Excerpta Medica] [Chemical Abstracts/CAS] [Index Copernicus]

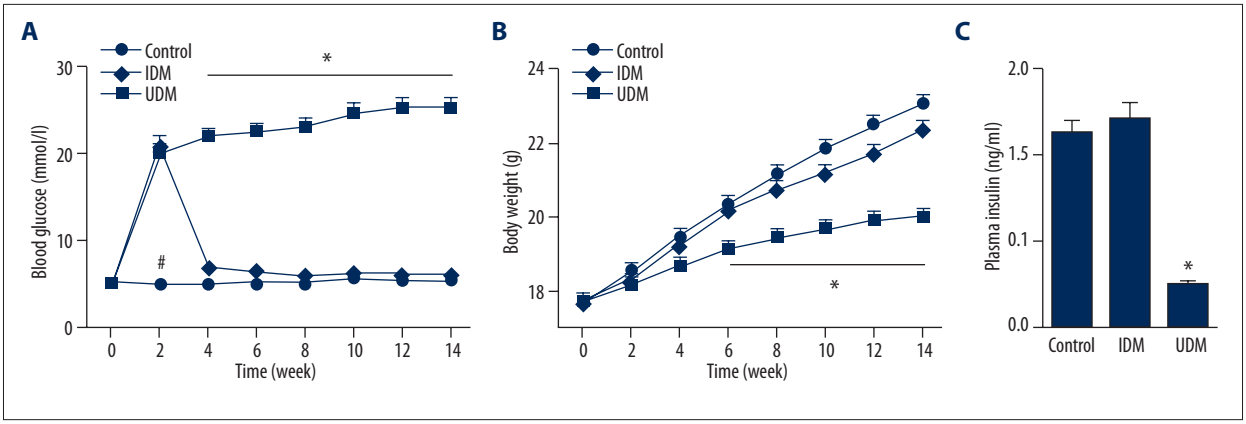

Figure 1. Blood glucose and plasma insulin levels of the control, IDM, and UDM groups. (**A**) Blood glucose of control, IDM, and UDM groups over 14 weeks. (**B**) Body weight of control, IDM, and UDM over 14 weeks. (**C**) Circulating plasma insulin level of control, IDM, and UDM groups at week 14. (n=20, * *P*<0.05 compared with control and IDM group; # *P*<0.05 compared with UDM and IDM group).

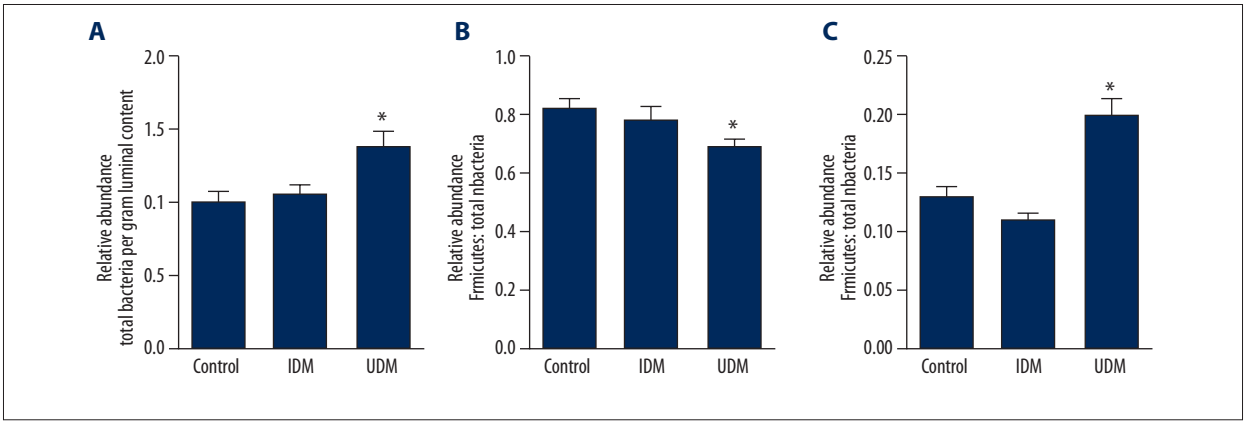

Figure 2. Intestinal bacterial load and relative abundance of *Firmicutes* and *Bacteroidetes* in the small intestine of control, IDM, and UDM mice. (**A**) Relative abundance of total bacteria per gram of luminal content in small intestines of the control, IDM, and UDM groups. (**B, C**) The relative abundance of *Firmicutes* (**B**) and *Bacteroidetes* (**C**) in small intestines of the control, IDM, and UDM groups (n=8, * *P*<0.05 compared with control and IDM groups).

the small intestine of the UDM group, and the insulin treatment normalized the gut microflora.

Intestinal bactericidal activity decreased in diabetic mice

The indicator strain of bacteria, *E. coli* K12, is a tetracycline-resistant bacterial strain. Compared to the control group, the exogenous bacteria recovered from the proximal and distal intestine of the UDM group were significantly increased (UDM group: $1.01\pm0.11\times10^6$ CFU/ml *vs.* control group: $4.12\pm0.61\times10^5$ CFU/ml in the proximal, n=10, *P*<0.05; UDM group: $3.57\pm0.99\times10^7$ CFU/ml *vs.* control group: $7.8\pm1.0\times10^6$ CFU/ml in the distal, n=10, *P*<0.05; Figure 3), but that of the IDM group was comparable to the control group (n=10, *P*>0.05; Figure 3). These findings suggest a defective innate defense in the intestines of diabetic mice.

Abnormal expression of anti-bacterial gene and protein in Paneth cells of diabetic mice

Paneth cells (Lyz^+ cells) were indicated by immunohistochemical staining in the crypts of control, IDM, and UDM groups at week 14 (Figure 4A). The quantification of Lyz^+ cells per crypt in the distant small intestine revealed a slight increase in the UDM group compared to the control and IDM groups (n=10, *P*<0.05; Figure 2B). As shown in Figure 4C, the percentage of Paneth cells ($CD24^{high}SSC^+$ cell) detected by flow cytometry in intestinal epithelial cells of the UDM group was significantly higher than that of the control group (1.12±0.12% *vs.* 0.74±0.06%; n=6, *P*<0.05; Figure 4C). The IDM group and the control group had the similar percentages of Paneth cells (n=6, *P*>0.05; Figure 4C).

Indexed in: [Current Contents/Clinical Medicine] [SCI Expanded] [ISI Alerting System] [ISI Journals Master List] [Index Medicus/MEDLINE] [EMBASE/Excerpta Medica] [Chemical Abstracts/CAS] [Index Copernicus]

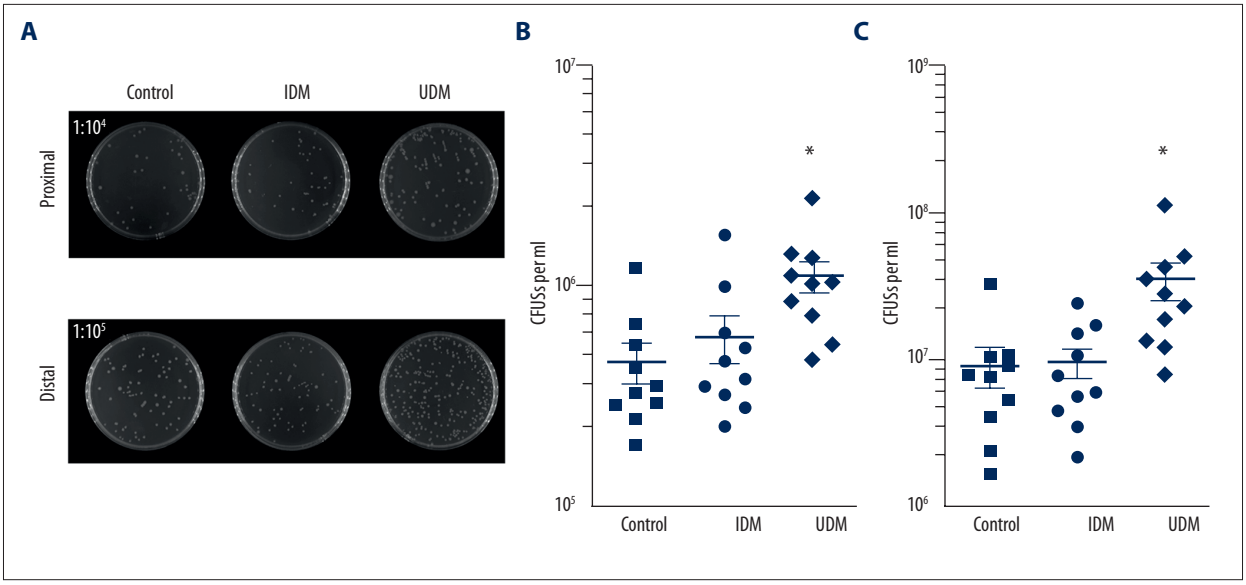

Figure 3. Intestinal bactericidal activity decreased in diabetic mice. (**A**) Representative plates of *E. coli* K12 recovered from the proximal and distal small intestines grown on LB media containing tetracycline (20 mg/l) are shown in this panel. (**B, C**) Compared to the control group, the exogenous bacteria recovered from the proximal (**B**) and distal (**C**) intestine of the UDM group were significantly increased (n=10, * $P<0.05$ compared with control and IDM group).

The mRNA expression of general Crps, matrix metallopeptidase 7 (Mmp7), and lysozyme 1 (Lyz1) in both the proximal and distant small intestines was lower in the UDM group (n=10, $P<0.05$; Figure 4D). Accordingly, the Lyz protein expression in the proximal and distant small intestines of the UDM group was significantly decreased compared with the control and IDM group (n=10, $P<0.05$; Figure 4E).

Decreased bactericidal activity of Paneth cells in small intestines of diabetic mice

To further explore the bactericidal function of Paneth cells in response to bacteria, the small intestinal crypts with specific appearance of Paneth cell granules and sheets of villi were isolated from the proximal and distal small intestines (Figure 5A). In this study, 10 ng/ml LPS was used to stimulate Paneth cells secretion, which was then assessed by the bactericidal assay using *E. coli* [8,31]. The primary Paneth cell secretion exhibited significantly reduced bactericidal activity after simulation with LPS *ex vivo* in the UDM group (21.7±1.9% in the proximal, 35.2±3% in the distal) than in the control group and the IDM group (n=10, $P<0.05$; Figure 5B). The IDM group failed to reach significance over the control group.

Increased mRNA expression of IR-A/IR-B ratio in Paneth cells of diabetic mice

As shown in Figure 6A, there were no significant changes in total IR levels of Paneth cells ($CD24^{high}SSC^{+}$ cell) in the 3 groups. Quantitative densitometry confirmed a significant increase in the IR-A/IR-B ratio in Paneth cells of the UDM group compared to the control group (n=6, $P<0.05$; Figure 6B). The control group and the IDM group had similar relative levels of IR-A/IR-B.

Effects of glucose, insulin, and mannitol treatment on anti-bacterial gene mRNA expression in crypt organoids

The primary mouse small intestinal crypts were isolated and cultured using a Matrigel-based culture system *in vitro* (Figure 7A). Without insulin treatment, higher glucose concentrations (11 mM and 22 mM) did not increase the mRNA expression of anti-bacterial genes (Crps, Mmp7, and Lyz1; Figure 7B). Insulin

Figure 4. Abnormal expressions of anti-bacterial gene and protein in Paneth cells of diabetic mice. (**A**) Paneth cells (arrowheads) were indicated by immunohistochemical staining for Lyz in the crypts of control, IDM, and UDM groups at week 14 (Bar indicates 25 μm). (**B**) The numbers of Paneth cells (Lyz^{+} cell) per crypt in the proximal (upper) and distal (down) small intestines among the 3 groups (n=10). (C) Flow cytometry was used to quantify Paneth cells ($CD24^{high}SSC^{+}$ cells) from the intestinal epithelium of individual groups (n=6). (**D**) mRNA expression of Crps, Mmp7, and Lyz1 in the proximal (upper) and distant (down) small intestines of control, IDM, and UDM groups (n=10). (**E**): Protein levels of Lyz indicated by Western blots in the proximal and distant small intestines of control, IDM, and UDM groups (n=10). (* $P<0.05$ compared with control and IDM group).

Indexed in: [Current Contents/Clinical Medicine] [SCI Expanded] [ISI Alerting System] [ISI Journals Master List] [Index Medicus/MEDLINE] [EMBASE/Excerpta Medica] [Chemical Abstracts/CAS] [Index Copernicus]

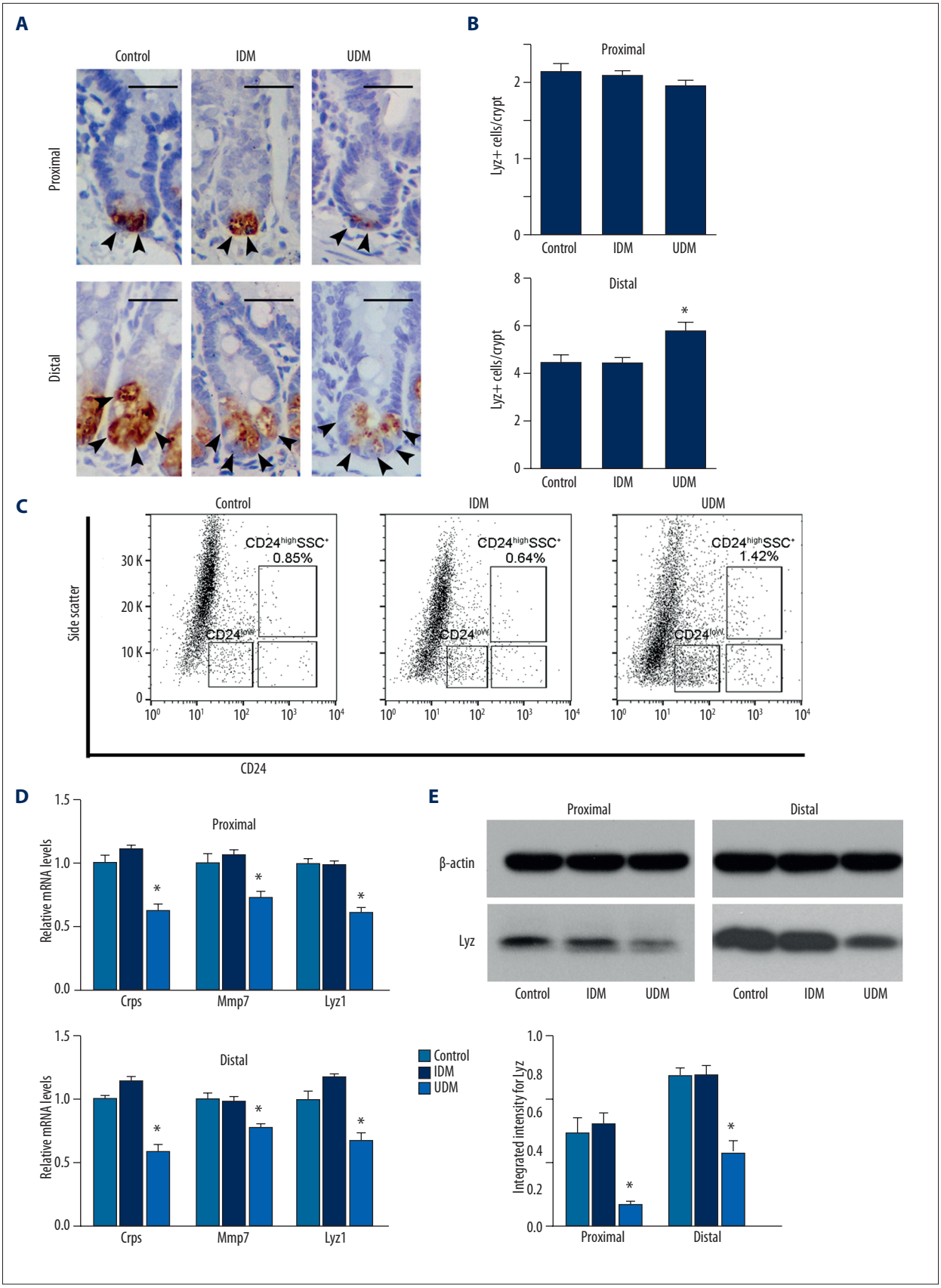

Indexed in: [Current Contents/Clinical Medicine] [SCI Expanded] [ISI Alerting System] [ISI Journals Master List] [Index Medicus/MEDLINE] [EMBASE/Excerpta Medica] [Chemical Abstracts/CAS] [Index Copernicus]

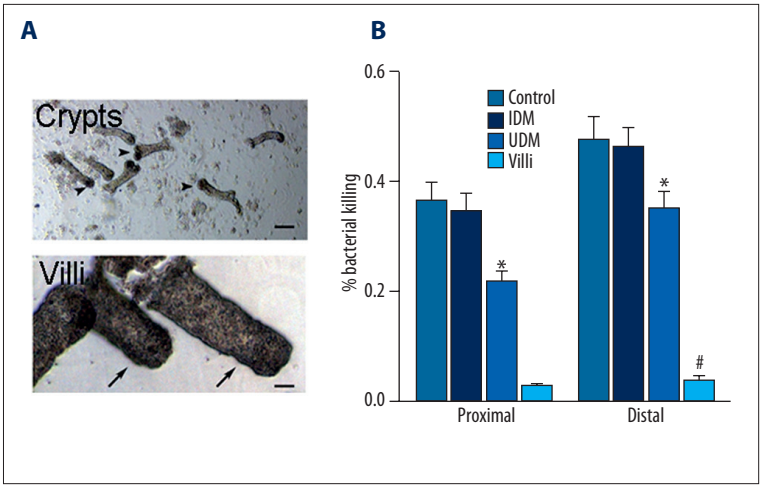

Figure 5. Decreased bactericidal activity of secretion from Paneth cells in diabetic mice. (**A**) Small intestinal crypts and villi were isolated by EDTA treatment from mice. Individual intact crypts (upper) are indicated by arrowheads and villi (lower) are indicated by arrows (Bar indicates 100 μm). (**B**) Bactericidal activity of secretion from Paneth cells of the proximal and distal intestines of the control, IDM, and UDM groups in response to LPS indicated by bacterial killing. Villi incubated with LPS were used be a control. (n=10, * P<0.05 compared with control and IDM groups, # P<0.05 compared with control, UDM, and IDM groups).

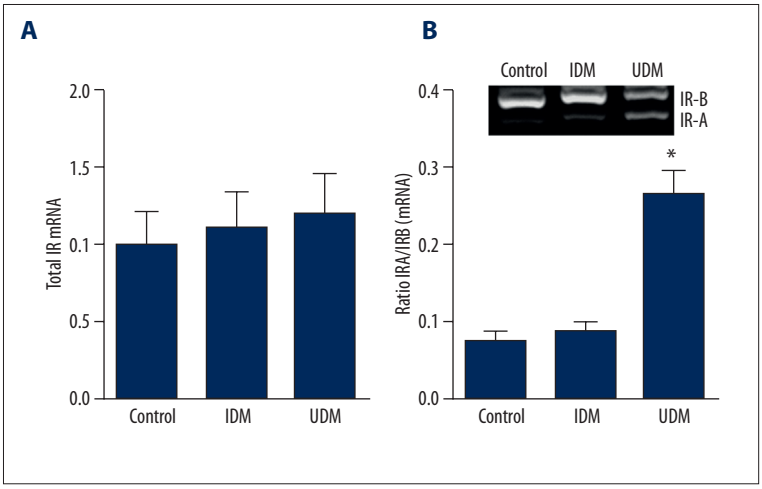

Figure 6. Increased relative levels of IR-A/IR-B in Paneth cells of diabetic mice. (**A**) Levels of total IR mRNA assayed by qRT-PCR on Paneth cells ($CD24^{high}SSC^{+}$ cells) isolated from small intestinal epithelium sorted by FACS (n=6). (**B**) The relative mRNA expression of IR-A/IR-B using primers spanning exon 11 of IR mRNA and quantitative analysis of IR-A/IR-B ratio of mRNA expression (n=6). (* P<0.05 compared with control and IDM groups).

treatment (100 nM) significantly increased the levels of anti-bacterial gene mRNA expression at 5.5 mM, 11 mM, and 22 mM glucose, whereas the mRNA expression of these genes in the 5.5-mM glucose condition was significantly higher than in the other 2 glucose conditions (n=6, P<0.05; Figure 7B).

To verify whether the osmotic property of glucose had an impact on the expression of anti-bacterial genes, mannitol was used instead of glucose. Mannitol did not lead to the upregulation of the expression of anti-bacterial genes (n=6; Figure 7C). In the 5.5-mM glucose condition, the mRNA expression of Crps, Mmp7, and Lyz1 in higher insulin concentrations (100 nM and 200 nM) was more significantly increased than that in the lower insulin concentration (10 nM; n=6, P<0.05; Figure 7D). However, 200 nM insulin did not further increase the expressions of these genes.

Discussion

T1DM has been associated with increased susceptibility to small bowel infection. The pathogenic mechanism is not clear. The establishment and preservation of beneficial interactions between the host and its associated intestinal microbiota have been increasingly acknowledged as key requirements for health. The disturbances in intestinal homeostasis have been linked to infectious diseases [32]. In the present study, the intestinal microflora and Paneth cells in T1DM mice were investigated.

Intestinal dysbiosis has been reported in many animal and human studies of T1DM. In previous studies, alterations in microflora have been hypothesized to contribute to the pathogenesis of T1DM [33,34]. However, we found that the progression of T1DM also had an impact on enteric bacteria. We used a STZ-induced diabetic mice model in which STZ damages pancreatic β cells, resulting in hypoinsulinemia and hyperglycemia (Figure 1) [35]. In this model, the intestinal bacterial load was increased in the UDM group (Figure 2A). In accordance with our

Indexed in: [Current Contents/Clinical Medicine] [SCI Expanded] [ISI Alerting System] [ISI Journals Master List] [Index Medicus/MEDLINE] [EMBASE/Excerpta Medica] [Chemical Abstracts/CAS] [Index Copernicus]

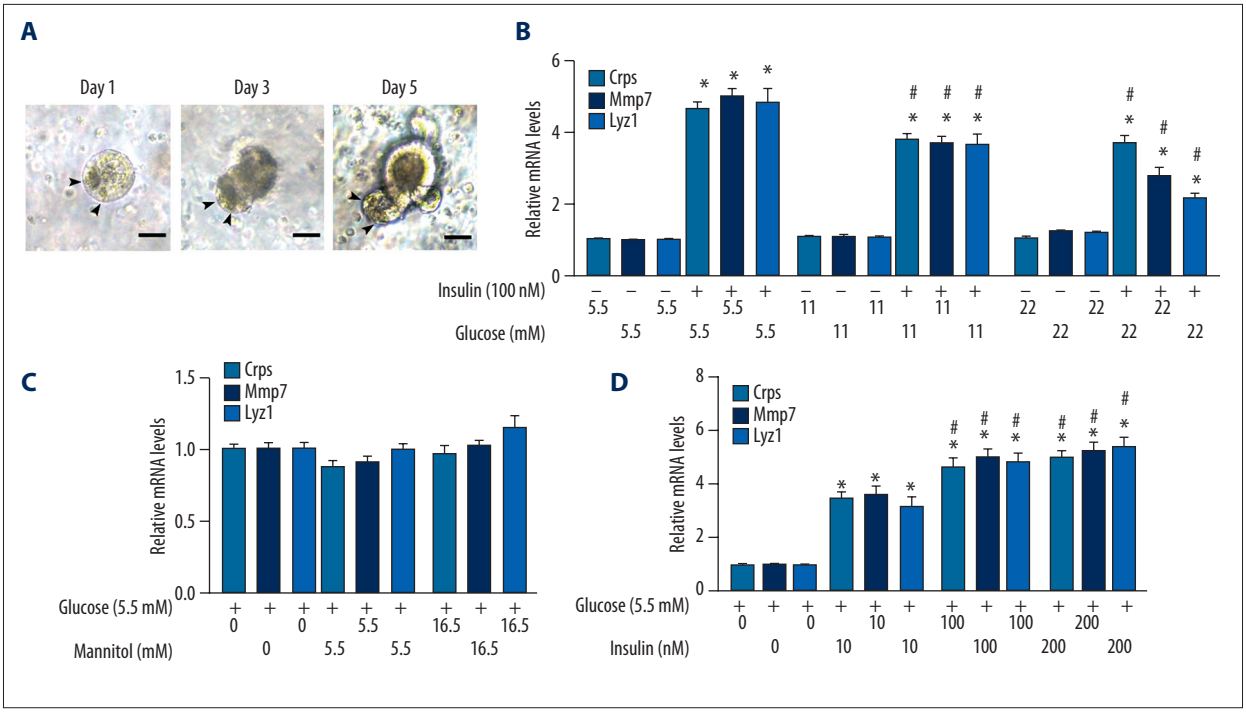

Figure 7. Effect of glucose, insulin, and mannitol treatment on anti-bacterial gene mRNA expression in crypt organoids. (**A**) Primary crypt organoids were cultured in a Matrigel-based culture system. Differential interference contrast image reveals granule-containing Paneth cells at crypt bottoms (arrowheads) (Bar indicates 100 μm). (**B**) The mRNA expression of Crps, Mmp7, and Lyz1 in crypt organoids cultured in different glucose concentrations (5.5 mM, 11 mM, and 22 mM) and without/with 100 nM insulin (insulin –/+) treatment (n=6, * P<0.05 compared with the condition in which crypt organoids were cultured in 5.5 mM glucose and without insulin, # P<0.05 compared with 5.5 mM glucose at the condition of insulin administration). (**C**) The mRNA expression of Crps, Mmp7, and Lyz1 in crypt organoids cultured in 5.5 mM glucose and different mannitol concentrations (0 mM, 5.5 mM, and 16.5 mM). (**D**) The mRNA expressions of Crps, Mmp7, and Lyz1 in 5.5 mM glucose and different insulin concentrations (0 nM, 10 nM, 100 nM, and 200 nM; n=6, * P<0.05 compared with 0 nM insulin condition; # P<0.05 compared with 10 nM insulin condition).

findings, Roza et al. showed that there was an overgrowth of mucosa-associated bacteria in the untreated diabetic gut [36]. In addition, the UDM group showed that relative abundances of *Firmicutes* were decreased and *Bacteroidetes* were increased (Figure 2B). These results revealed qualitative and quantitative changes in the microflora in the small intestine of the UDM group. In our study, the main microbiota composition was analyzed at the phylum level. It would be interesting to investigate the dysbiosis of diabetic mice at a lower level in the future. The intestinal dysbiosis represented imbalances between the host and microbiota. In addition, exogenous *E. coli* survived much more easily in the small bowel of untreated diabetic mice. At 3 h after inoculation of bacteria, the intestinal innate immune system played the major role in defending against exogenous bacteria. Therefore, we suggest that in the UDM group, the intestinal bactericidal activity decreased, which suggests inadequacy in the intestinal innate immune system and more risks of small bowel infection, resulting in the dysbiosis.

What factor changed the intestinal innate immune system of the UDM group? It is well known that Paneth cells play a key role in intestinal innate mucosal immunity [5]. Here, we reported the dysfunction of Paneth cells in the long-term T1DM mice for up to 14 weeks. In our study, the expression of Paneth cell-derived antimicrobial genes (Crps, Mmp7, and Lyz) was significantly reduced in the UDM group compared with the control group, and the secretion of Paneth cells stimulated by LPS decreased in the UDM group (Figure 4). To recapitulate, our results show that the dysbiosis observed in the UDM group coincided with the dysfunction of Paneth cells in diabetic mice.

Intestinal microbiota and Paneth cells are closely associated, both mutually affecting each other. In normal conditions, abnormal overgrowth of lumen bacteria can promote the production and export of Paneth cell-derived anti-microbial peptides [31]. Conversely, in the UDM group, this interplay has been shown to operate in the other direction. Therefore, we believe that the dysfunction of Paneth cells occurred prior to the alteration of the intestinal microbiota, and the latter was an adaptive response to changes in Paneth cells secretion present in the lumen. However, future studies may improve knowledge of the effect of Paneth cells on the dysbiosis of diabetic mice.

Indexed in: [Current Contents/Clinical Medicine] [SCI Expanded] [ISI Alerting System] [ISI Journals Master List] [Index Medicus/MEDLINE] [EMBASE/Excerpta Medica] [Chemical Abstracts/CAS] [Index Copernicus]

Salzman et al. demonstrated that a deficiency in cryptdin resulted in changes in microbiota composition, but not in total bacterial numbers [6]. However, in our study, both the bacterial load and the major bacterial microbiome constituents were changed in the luminal content of the UDM group. Decreased expression of both Crps and Lyz in Paneth cells might result in the defective intestinal innate immunity system of the UDM group, further supported by reduced bactericidal activity of Paneth cell *ex vivo*, leading to qualitative and quantitative changes in the intestinal flora. It appears that there was a synergistic effect between Crps and Lyz in establishing and maintaining the intestinal microbiota.

Several studies have reported that the number of Paneth cells increased in diabetic intestines [37,38]. This was further confirmed by the analysis of immunohistochemistry and flow cytometry in our study. Interestingly, the expression of Paneth cell-derived antimicrobial peptides exhibited the inverse trend (Figure 4). This paradoxical phenomenon illustrates the inadequate maturation of Paneth cells in the UDM group while proliferation increased. Our previous work showed that the Notch/Hes1 signal pathway was depressed in diabetic mice [39]. The inactivity of the Notch/Hes1 signal pathway can induce differentiation of intestinal stem cells into secretory lineages, including Paneth cells [40]. Therefore, the increased number of Paneth cells may be the consequence of the depressed Notch/Hes1 signal pathway. Once specified, Paneth cells undergo the MMP-7/Crps maturation program activated by the Wnt signaling pathway, but expression of Lyz is independent of the Wnt signaling pathway [17]. The reduced expression of Crps, Mmp7, and Lyz in diabetic mice indicates that the Wnt signaling pathway may not be the only mechanism involved in the maturity of Paneth cells. This remains to be further explored.

Andres et al. showed that IR-A and IR-B isoforms are expressed in a gradient from proliferative stem and progenitor cells to differentiated lineages along the crypt-villus axis [41]. IR-A enhances cell proliferation, and IR-B mediates differentiation and metabolism [29,42]. In our study, we found that relative levels of IR-A/IR-B in Paneth cells of the UDM group were elevated, but the total IR mRNA expression was not changed (Figure 6). This may reflect the immature status of Paneth cells in the UDM group, which is consistent with the impaired bactericidal function of Paneth cells (Figures 4 and 5), but it is unclear whether the IR signal pathway mediates differentiation or maturity of Paneth cells.

In our work, insulin treatment normalized blood glucose and body weight in diabetic mice (Figure 1). The number of Paneth cells, the levels of the mRNA and protein of Paneth cell-derived antimicrobial peptides, the bactericidal activity of Paneth cell secretions, and the relative expression of IR-A/IR-B in the diabetic gut were restored by injection of exogenous insulin (Figures 4–6). We postulated that deficiency of endogenous insulin might impair the bactericidal function of Paneth cells during diabetes, resulting in attenuation of the innate immunity of the small intestine and leading to altered intestinal flora.

The primary mouse small intestinal crypt culture *in vitro* was conducted to test whether insulin had an influence on the expression of Paneth cell-derived antibacterial protein (Figure 7A). In the absence of insulin with different glucose concentrations, Paneth cell-derived antimicrobial peptides were expressed at relatively low and stable levels, but insulin supplementation (100 nM) significantly enhanced their expression. This suggests that insulin rather than glucose is needed for the optimal expression of antimicrobial peptides in Paneth cells. These results were in agreement with the *in vivo* finding that insulin treatment normalized the expression of anti-bacterial genes in diabetic mice. At higher glucose concentrations (11 mM and 22 mM) in the presence of 100 nM insulin, lower expression of these genes was achieved compared with lower glucose concentration (5.5 mM; Figure 7). These findings indicate that higher glucose concentrations may lead to some degree of insulin resistance. Furthermore, mannitol instead of glucose had no impact on the expression of these genes, which demonstrates that the expression of anti-bacterial genes at elevated glucose concentrations with insulin treatment is not affected by the osmotic property of glucose.

The average blood glucose level was 5.5 mM, which is controlled by insulin *in vivo*. At 5.5 mM glucose condition, higher insulin concentrations further increased the expression of Paneth cell-derived antimicrobial peptides in the Matrigel-based culture system. In our experiment, the highest levels of the expression of these genes were achieved with 100 nM insulin (Figure 7). Conclusively, these data emphasize the importance of insulin for anti-bacterial gene expression in the small intestine.

Our findings suggest that insulin is essential to the optimal expression of antimicrobial peptides in Paneth cells. In other systems, insulin is known to activate β-catenin/TCF, downstream mediators of the Wnt signal pathway [12,43]. In addition, it has been shown that the influence of insulin on different intestinal epithelial cell types varies depending on relative IR-A/IR-B expression levels [41]. Consequently, it is possible that with deficiency of insulin and increased relative levels of IR-A/IR-B, Paneth cells in diabetic mice could not reach full maturity, resulting in low expression of antimicrobial peptides.

Conclusions

Our study shows the bactericidal function of intestinal Paneth cells was impaired in STZ-induced diabetic mice, resulting in altered intestinal flora. We also provide evidence that the deficiency of insulin results in the immaturity of Paneth cells. Our

Indexed in: [Current Contents/Clinical Medicine] [SCI Expanded] [ISI Alerting System] [ISI Journals Master List] [Index Medicus/MEDLINE] [EMBASE/Excerpta Medica] [Chemical Abstracts/CAS] [Index Copernicus]

primary mouse intestinal crypt culture further demonstrated that insulin was essential for the optimal expression of Paneth cell-derived antimicrobial peptides.

References:

1. Telzak EE, Greenberg MS, Budnick LD et al: Diabetes mellitus – a newly described risk factor for infection from *Salmonella enteritidis*. J Infect Dis, 1991; 164(3): 538–41
2. Oikarinen M, Tauriainen S, Honkanen T et al: Detection of enteroviruses in the intestine of type 1 diabetic patients. Clin Exp Immunol, 2008; 151(1): 71–75
3. Gosiewski T, Salamon D, Szopa M et al: Quantitative evaluation of fungi of the genus Candida in the feces of adult patients with type 1 and 2 diabetes – a pilot study. Gut Pathog, 2014; 6(1): 43
4. Duerkop BA, Vaishnava S, Hooper LV: Immune responses to the microbiota at the intestinal mucosal surface. Immunity, 2009; 31(3): 368–76
5. Ouellette AJ: Paneth cells and innate mucosal immunity. Curr Opin Gastroenterol, 2010; 26(6): 547–53
6. Salzman NH, Hung K, Haribhai D et al: Enteric defensins are essential regulators of intestinal microbial ecology. Nat Immunol, 2010; 11(1): 76–83
7. Wilson CL: Regulation of intestinal – defensin activation by the metalloproteinase matrilysin in innate host defense. Science, 1999; 286(5437): 113–17
8. Lee SJ, Lee J, Li KK et al: Disruption of the murine Glp2r impairs Paneth cell function and increases susceptibility to small bowel enteritis. Endocrinology, 2012; 153(3): 1141–51
9. Kobayashi KS, Chamaillard M, Ogura Y et al: Nod2-dependent regulation of innate and adaptive immunity in the intestinal tract. Science, 2005; 307(5710): 731–34
10. Salzman NH, Ghosh D, Huttner KM et al: Protection against enteric salmonellosis in transgenic mice expressing a human intestinal defensin. Nature, 2003; 422(6931): 522–26
11. Yi F, Sun J, Lim GE et al: Cross talk between the insulin and Wnt signaling pathways: Evidence from intestinal endocrine L cells. Endocrinology, 2008; 149(5): 2341–51
12. Sun J, Khalid S, Rozakis-Adcock M et al: P-21-activated protein kinase-1 functions as a linker between insulin and Wnt signaling pathways in the intestine. Oncogene, 2009; 28(35): 3132–44
13. Sun J, Wang D, Jin T: Insulin alters the expression of components of the Wnt signaling pathway including TCF-4 in the intestinal cells. Biochim Biophys Acta, 2010; 1800(3): 344–51
14. Yilmaz OH, Katajisto P, Lamming DW et al: mTORC1 in the Paneth cell niche couples intestinal stem-cell function to calorie intake. Nature, 2012; 486(7404): 490–95
15. Gregorieff A, Pinto D, Begthel H et al: Expression pattern of Wnt signaling components in the adult intestine. Gastroenterology, 2005; 129(2): 626–38
16. Korinek V, Barker N, Moerer P et al: Depletion of epithelial stem-cell compartments in the small intestine of mice lacking Tcf-4. Nat Genet, 1998; 19(4): 379–83
17. van Es JH, Jay P, Gregorieff A et al: Wnt signalling induces maturation of Paneth cells in intestinal crypts. Nat Cell Biol, 2005; 7(4): 381–86
18. Batlle E, Henderson JT, Beghtel H et al: Beta-catenin and TCF mediate cell positioning in the intestinal epithelium by controlling the expression of EphB/ephrinB. Cell, 2002; 111(2): 251–63
19. Ma J, Phillips L, Wang Y et al: Curcumin activates the p38MPAK-HSP25 pathway *in vitro* but fails to attenuate diabetic nephropathy in DBA2J mice despite urinary clearance documented by HPLC. BMC Complement Altern Med, 2010; 10: 67
20. Chatzigeorgiou A, Halapas A, Kalafatakis K, Kamper E: The use of animal models in the study of diabetes mellitus. In vivo, 2009; 23(2): 245–58
21. Pei H, Qu Y, Lu X et al: Cardiac-derived adiponectin induced by long-term insulin treatment ameliorates myocardial ischemia/reperfusion injury in type 1 diabetic mice via AMPK signaling. Basic Res Cardiol, 2013; 108(1): 322
22. Zabielski P, Blachnio-Zabielska A, Lanza IR et al: Impact of insulin deprivation and treatment on sphingolipid distribution in different muscle subcellular compartments of streptozotocin-diabetic C57Bl/6 mice. Am J Physiol Endocrinol Metab, 2014; 306(5): E529–42
23. Bacchetti De Gregoris T, Aldred N et al: Improvement of phylum- and class-specific primers for real-time PCR quantification of bacterial taxa. J Microbiol Methods, 2011; 86(3): 351–56
24. Kimura I, Ozawa K, Inoue D et al: The gut microbiota suppresses insulin-mediated fat accumulation via the short-chain fatty acid receptor GPR43. Nat Commun, 2013; 4: 1829
25. Bjerknes M, Cheng H: Methods for the isolation of intact epithelium from the mouse intestine. Anat Rec, 1981; 199(4): 565–74
26. von Furstenberg RJ, Gulati AS, Baxi A et al: Sorting mouse jejunal epithelial cells with CD24 yields a population with characteristics of intestinal stem cells. Am J Physiol Gastrointest Liver Physiol, 2011; 300(3): G409–17
27. Sato T, van Es JH, Snippert HJ et al: Paneth cells constitute the niche for Lgr5 stem cells in intestinal crypts. Nature, 2011; 469(7330): 415–18
28. Gulati AS, Shanahan MT, Arthur JC et al: Mouse background strain profoundly influences Paneth cell function and intestinal microbial composition. PloS One, 2012; 7(2): e32403
29. Ulanet DB, Ludwig DL, Kahn CR, Hanahan D: Insulin receptor functionally enhances multistage tumor progression and conveys intrinsic resistance to IGF-1R targeted therapy. Proc Natl Acad Sci USA, 2010; 107(24): 10791–98
30. Sato T, Vries RG, Snippert HJ et al: Single Lgr5 stem cells build crypt-villus structures *in vitro* without a mesenchymal niche. Nature, 2009; 459(7244): 262–65
31. Ayabe T, Satchell DP, Wilson CL et al: Secretion of microbicidal alpha-defensins by intestinal Paneth cells in response to bacteria. Nat Immunol, 2000; 1(2): 113–18
32. Cerf-Bensussan N, Gaboriau-Routhiau V: The immune system and the gut microbiota: friends or foes? Nat Rev Immunol, 2010; 10(10): 735–44
33. Vaarala O: Gut microbiota and type 1 diabetes. Rev Diabet Stud, 2012; 9(4): 251–59
34. Dunne JL, Triplett EW, Gevers D et al: The intestinal microbiome in type 1 diabetes. Clin Exp Immunol, 2014; 177(1): 30–37
35. Leiter EH: Multiple low-dose streptozotocin-induced hyperglycemia and insulitis in C57BL mice: influence of inbred background, sex, and thymus. Proc Natl Acad Sci USA, 1982; 79(2): 630–34
36. Roza AM, Edmiston CE Jr., Frantzides C et al: Untreated diabetes mellitus promotes intestinal microbial overgrowth. Am J Surg, 1992; 163(4): 417–21
37. Ettarh RR, Carr KE: A morphological study of the enteric mucosal epithelium in the streptozotocin-diabetic mouse. Life Sci, 1997; 61(18): 1851–58
38. Thulesen J, Hartmann B, Nielsen C et al: Diabetic intestinal growth adaptation and glucagon-like peptide 2 in the rat: Effects of dietary fibre. Gut, 1999; 45(5): 672–78
39. Min XH, Yu T, Qing Q et al: Abnormal differentiation of intestinal epithelium and intestinal barrier dysfunction in diabetic mice associated with depressed Notch/NICD transduction in Notch/Hes1 signal pathway. Cell Biol Int, 2014; 38(10): 1194–204
40. Noah TK, Shroyer NF: Notch in the intestine: Regulation of homeostasis and pathogenesis. Ann Rev Physiol, 2013; 75: 263–88
41. Andres SF, Mah AT, Agostina Santoro M et al: Insulin receptor isoform switching in intestinal stem cells, progenitors, differentiated lineages and tumors: Evidence that IR-B limits proliferation. J Cell Sci, 2013; 126(Pt 24): 5645–56
42. Bortvedt S, Mah A, Van Landeghem L et al: Insulin receptor isoform B is downregulated in intestinal stem cells and tumors, limits colon cancer cell growth, and promotes differentiation. Faseb J, 2013; 27: 1
43. Dearth RK, Cui X, Kim HJ et al: Mammary tumorigenesis and metastasis caused by overexpression of insulin receptor substrate 1 (IRS-1) or IRS-2. Mol Cell Biol, 2006; 26(24): 9302–14

Conflict of interest

There is no conflict of interest to be declared

Indexed in: [Current Contents/Clinical Medicine] [SCI Expanded] [ISI Alerting System] [ISI Journals Master List] [Index Medicus/MEDLINE] [EMBASE/Excerpta Medica] [Chemical Abstracts/CAS] [Index Copernicus]